TECHNICAL MEMORANDUM

568

Comparison of river basin hydrometeorology in ERA-Interim and ERA-40 with observations

Alan K. Betts[1], Martin Köhler and Yuanchong Zhang[2]

Research Department

[1]Atmospheric Research, Pittsford, Vermont
[2]NASA GISS, New York, New York

Submitted to JGR

July 2008

European Centre for Medium-Range Weather Forecasts
Europäisches Zentrum für mittelfristige Wettervorhersage
Centre européen pour les prévisions météorologiques à moyen terme

Series: ECMWF Technical Memoranda

A full list of ECMWF Publications can be found on our web site under:
http://www.ecmwf.int/publications/

Contact: library@ecmwf.int

Abstract

The changes between the ERA-40 and ERA-Interim reanalyses in the seasonal cycle of primarily temperature, precipitation and evaporation, the surface radiation budget and the cloud fields are evaluated over three river basins, the Amazon, Mississippi and Mackenzie, for the period 1990-2001, using a variety of surface observational datasets and the ISCCP data. In ERA-Interim over the Amazon, the unrealistic interannual drift of precipitation has been reduced, and annual precipitation is largely unbiased, although the seasonal amplitude of precipitation remains too small. However, ERA-Interim has a large cold 2-m temperature bias. The clear-sky surface shortwave flux in ERA-Interim is lower than in ERA-40, and closer to observations. Low cloud cover has increased dramatically in ERA-Interim, and total reflective cloud cover has a larger positive bias in comparison with observations. The ratio of the surface short wave cloud forcing to the precipitation heating of the atmosphere is much lower in the observations than both reanalyses. The diurnal cycle of precipitation has improved somewhat with the removal of a spurious early morning peak. For the Mississippi and Mackenzie, the spinup of precipitation in 24h forecasts has been greatly reduced. Temperature biases are small in both reanalyses, but summer precipitation and evaporation exceed observational estimates. For the Mississippi, reflective cloud cover in ERA-Interim has increased in winter and decreased in summer compared with ERA-40, giving a closer fit to the observations in both seasons. For the Mackenzie, similar reflective cloud changes in ERA-Interim improve the fit to the observations in summer but not in winter.

1 Introduction

The hydrometeorology in ERA-40 (Uppala et al., 2005) of three American river basins, the Amazon, Mississippi and Mackenzie Rivers, was compared against observations by Betts et al. (2003a, b, 2005). They found substantial drifts over the 45 years of the ERA-40 reanalysis, associated with changes in the observational data; and with difficulties in the assimilation of the satellite data in recent decades (Andersson et al., 2005; Simmons et al., 2004). The spinup of the dynamic fields and precipitation in the first 24h was also substantial in mid-latitudes. Over the Amazon, there was a spurious early morning peak in the diurnal cycle of precipitation (Betts and Jakob, 2002); and long-term trends in the water cycle could not be determined, because of the drifts in column water vapor and precipitation (Hagemann et al., 2005). The biases in 2-m temperature on river basin scales in the 1990s were however small. A later paper (Betts, 2007) showed that ERA-40 has a low bias in reflective cloud cover over the Mississippi in all seasons except summer. A new interim reanalysis (ERA-Interim, which we shall abbreviate as ERA-Interim in the Figures), with improved variational bias correction of the satellite observations, and using a more recent cycle of the ECMWF model, was initiated for the period 1989-present. This paper presents some of the differences in the land-surface climate between the two reanalyses averaged over the Amazon, Mississippi and Mackenzie River basins for their overlap period.

1.1 Model Changes

There are substantial differences between the models used for these two reanalyses. ERA-40, a 3-D variational assimilation system, used model cycle 23R4, at a horizontal resolution of T_L-159 with 60 levels in the vertical. ERA-Interim is a 4-D variational assimilation system, running model cycle 31R2 at a horizontal resolution of T_L-255 with the same 60 levels in the vertical. The extensive model changes between cycle 23R4 in June 2001 and cycle 31R2 in December 2006 are listed at
http://www.ecmwf.int/products/data/technical/model_id.

The data assimilation changes include a completely revised humidity analysis, wavelet-based background error covariances and variational bias correction of radiance data, which results in a much reduced unrealistic drift in the hydrological cycle (Simmons et al., 2006; Uppala et al., 2008). The model physics changes are substantial

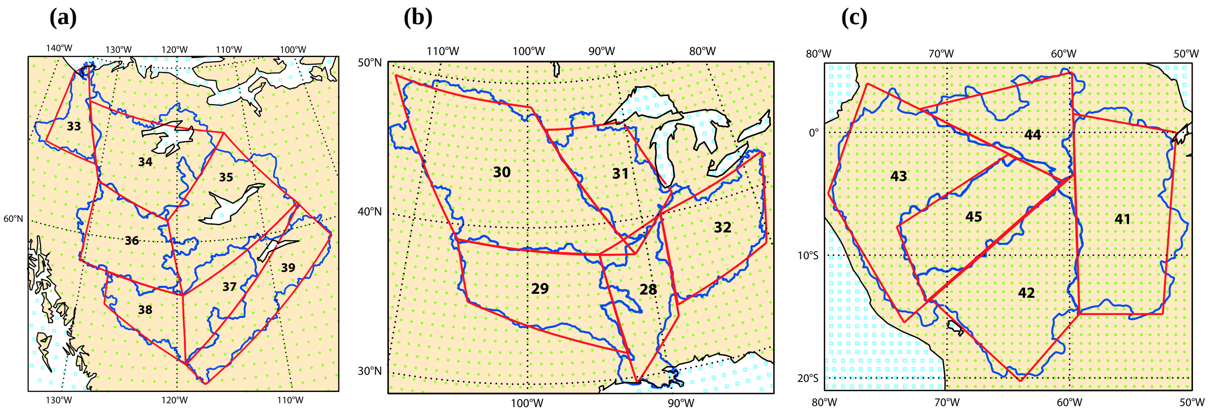

Figure 1: Mackenzie (a), Mississippi (b) and Amazon (c) river basins selected from ERA-40 and ERA-Interim hourly archives.

between the two reanalyses. Tompkins et al. (2004) gives a detailed review of the model changes in moist physics from ERA-40 up to cycle 28R3. There are changes to the cloud, convection (Bechtold et al., 2004) and boundary layer schemes (Köhler, 2005), a new treatment of orographic drag (Beljaars et al., 2003), a new shortwave radiative transfer scheme and a new aerosol climatology (Morcrette et al., 2007). The tiled land-surface model, acronym TESSEL (Van den Hurk et al., 2000), has changed very little between ERA-40 and ERA-Interim, and specifically the snow and hydrology models have not been revised. As a result, ERA-Interim has the same early snow melt error as ERA-40, and no surface runoff, except over frozen ground; so these aspects of the surface hydrology will not be discussed here.

1.2 River basin archive

The ECMWF reanalyses archive (Kållberg et al., 2004) contains averages, at an hourly time frequency, over many river basins around the globe. Figure 1 shows the three river basins that we use in this paper: from top to bottom the Mackenzie, Mississippi and Amazon. Each is divided into sub-basins, with the hydrological boundaries as shown, and each sub-basin is approximated in the reanalyses by averages over all grid-points within the numbered red quadrilaterals. These are labeled 33-39 for the Mackenzie, 28-32 for the Mississippi and 41-45 for the Amazon. The grid-points shown are for ERA-Interim. We use two products. For the broad seasonal cycle comparisons, we use monthly averages over the three large basins, derived from the 6-30h forecasts from the 00 UTC analysis. ERA-40 ended in August 2002, and ERA-Interim began in 1989, so the primary overlap period we have chosen for comparison is 1990-2001. From the twelve years, four months have substantial missing data in this ERA-Interim river basin archive and we have been omitted them from our analysis, but the impact of doing this is very small. To compare the diurnal cycles and some aspects of the daily cloud statistics, we shall use the sub-basins for the year 1994. For this we have 36h forecasts from both the 00 and 12 UTC analyses, so we can also compare the spinup of precipitation in the first 36h.

1.3 Observations

This paper illustrates differences in the land-surface climate between the two reanalyses, and is focused on a few variables: temperature, humidity, precipitation and evaporation, radiation and cloud fields. We shall use for comparison primarily the same observations used in previous papers (Betts et al., 2003a, b, 2005), coming from various sources. For the Amazon, the monthly and seasonal means come from Jones and Moberg (2003), Dai et

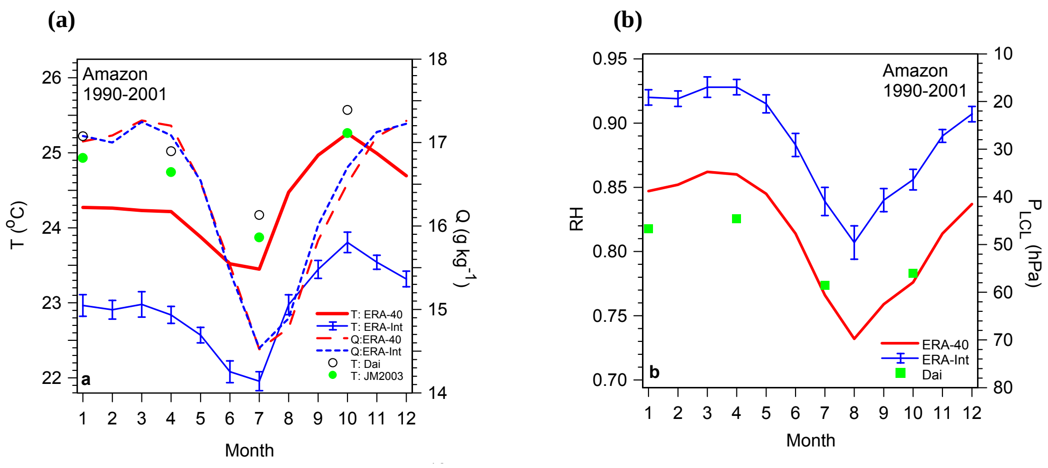

Figure 2: Mean annual cycle of (a) 2-m temperature and specific humidity; (b) 2-m RH and pressure height to LCL.

al. (2004) and Dai (2006), and the period 1990-2001 is covered. For the Mississippi, our monthly dataset comes from the hydrological analysis of Maurer et al. (2002), and for these data we have only the years 1990-1999 for comparison. We shall also use a daily precipitation mean for 1994 from Betts (2007). For the Mackenzie River, we use the observations processed (Louie et al., 2002) for the Mackenzie GEWEX Study, MAGS (see Woo et al., 2008), which cover the eight years, 1990-1997, for temperature and precipitation, and 1990-1996 for evaporation. For our analysis of the systematic changes in the land-surface climate between ERA-40 and ERA-Interim, the small differences in time period extent for the many different datasets is not signifi cant.

For the incoming short-wave radiation and an estimate of the short-wave cloud albedo, we use data from the International Satellite Cloud Climatology Project, ISCCP (Rossow and Zhang, 1995; Zhang et al., 1995, 2004, 2006, 2007), averaged over the same river basins in Figure 1. This time-series, with a 3-hrly time resolution, covers the period July, 1983 to December, 2006; and we will use the 12 years, 1990-2001 for this study.

2 Annual cycle for river basins

2.1 Amazon Basin

Figure 2 (a) compares the basin-mean annual cycle of 2-m temperature, T, and specifi c humidity, Q, from ERA-40 and ERA-Interim with a basin-mean derived from surface observations. The error bars on ERA-Interim in both panels are the standard deviations of the monthly mean differences between the two reanalyses. ERA-Interim is 1.4K cooler than ERA-40, which was already a little cooler than the two observational estimates shown (seasonal means from Dai et al. (2004), Dai (2006) and Jones and Moberg (2003), abbreviated JM2003). Specifi c humidity is little changed between the two reanalyses. Figure 2(b) shows the comparison of 2-m relative humidity, RH, and the corresponding pressure height of the lifting condensation level, PLCL (with slight approximation). ERA-Interim has a surface RH that is about 7% higher throughout the year with a corresponding mean LCL, almost 20 hPa lower. This is a signifi cant drop in mean cloud-base. Again ERA-40 is closer to the observations than ERA-Interim.

Figure 3 (upper curves) compares the annual cycle of precipitation (from the 6-30h forecast from the 00 UTC analysis) with an observational estimate from Dai et al. (2004). The standard deviations (only shown for the data) of the interannual variability of monthly precipitation of data and reanalyses are similar: about ± 0.3 mm day^{-1} in the dry season and ± 0.6 mm day^{-1} in the rainy season. The lower curves are the differences

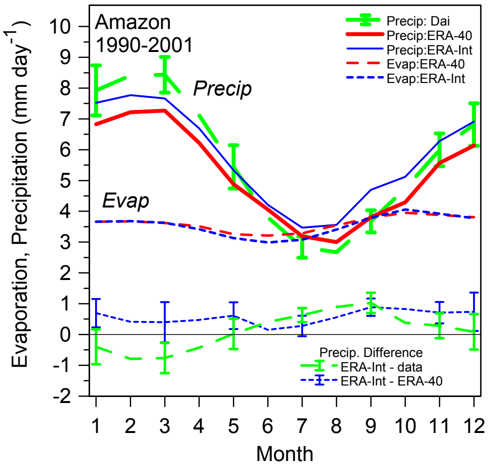

Figure 3: Annual cycle of precipitation and evaporation for the Amazon basin.

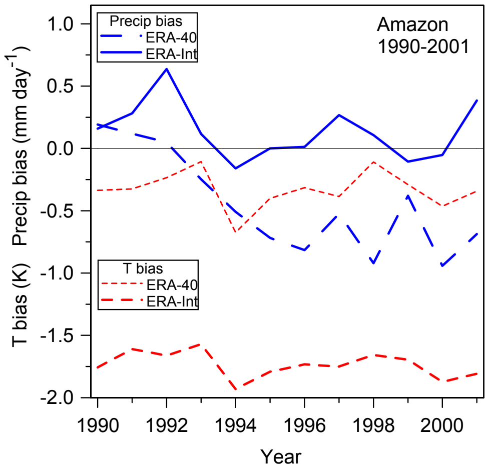

Figure 4: Mean annual bias of temperature and precipitation for the Amazon basin.

of ERA-Interim from ERA-40 and the observations. ERA-Interim has more precipitation in all seasons than ERA-40, which reduces the dry bias in the rainy season, but increases the model wet bias in the dry season. Evaporation, which has very little interannual variability ($\pm$0.1 mm day^{-1}) is slightly lower in the dry season in ERA-Interim, and we shall see later in Figure 5(c) that this is associated with a drop in surface net radiation. With increased precipitation and reduced evaporation, ERA-Interim has increased deep runoff (not shown).

Figure 4 shows the mean annual temperature and precipitation bias of ERA-40 and ERA-Interim from the observations. For temperature, the much larger cold bias in ERA-Interim is again visible, and the interannual variability of the bias is small. For precipitation, the bias in ERA-Interim is smaller than in ERA-40; which shows an unrealistic negative drift in the bias during these years, as noted in earlier work (Betts et al., 2005). It appears that the improved variational bias correction of the satellite observations in ERA-Interim has successfully reduced the drift of precipitation over the Amazon during this period (Uppala et al., 2008).

Figure 5 shows several aspects of the radiation balance and cloud cover. Figure 5(a) shows that the clear-sky and all-sky downward shortwave fluxes, SW_{down}, are substantially lower in ERA-Interim than ERA-40. The atmospheric shortwave reflection is greater in ERA-Interim than ERA-40, and in the dry season (June to August) the downwelling shortwave clear-sky flux has decreased by 16 Wm^{-2}. The ISCCP calculation of the clear-sky flux (Zhang et al., 2004) agrees with ERA-40 in the rainy season and ERA-Interim in the dry season. The standard deviations (not shown) of the interannual variability of the clear-sky fluxes are small for the ISCCP data ($\approx$ 2 Wm^{-2}), which estimates atmospheric aerosols; and tiny for the reanalyses ($\approx$ 0.5 Wm^{-2}), where an aerosol climatology is specified. Figure 5(a) also shows the surface all-sky SW_{down} estimate from the ISCCP dataset (Zhang et al., 2004). In comparison with the ISCCP estimate, both the reanalyses have less incoming shortwave radiation at the surface during the November to May rainy season. ERA-40 agrees with ISCCP only during the dry season in August, when ERA-40 has a higher clear-sky flux, so it is clear there must be substantial differences in the shortwave cloud forcing.

A useful non-dimensional measure of the surface shortwave cloud forcing was proposed by Betts and Viterbo (2005) and Betts (2007). We derive an effective cloud albedo from the surface short-wave cloud forcing, SWCF, as

$$\alpha_{cloud} = -SWCF/SW_{down}(Clear) \tag{1}$$

where

$$SWCF = SW_{down} - SW_{down}(Clear) \tag{2}$$

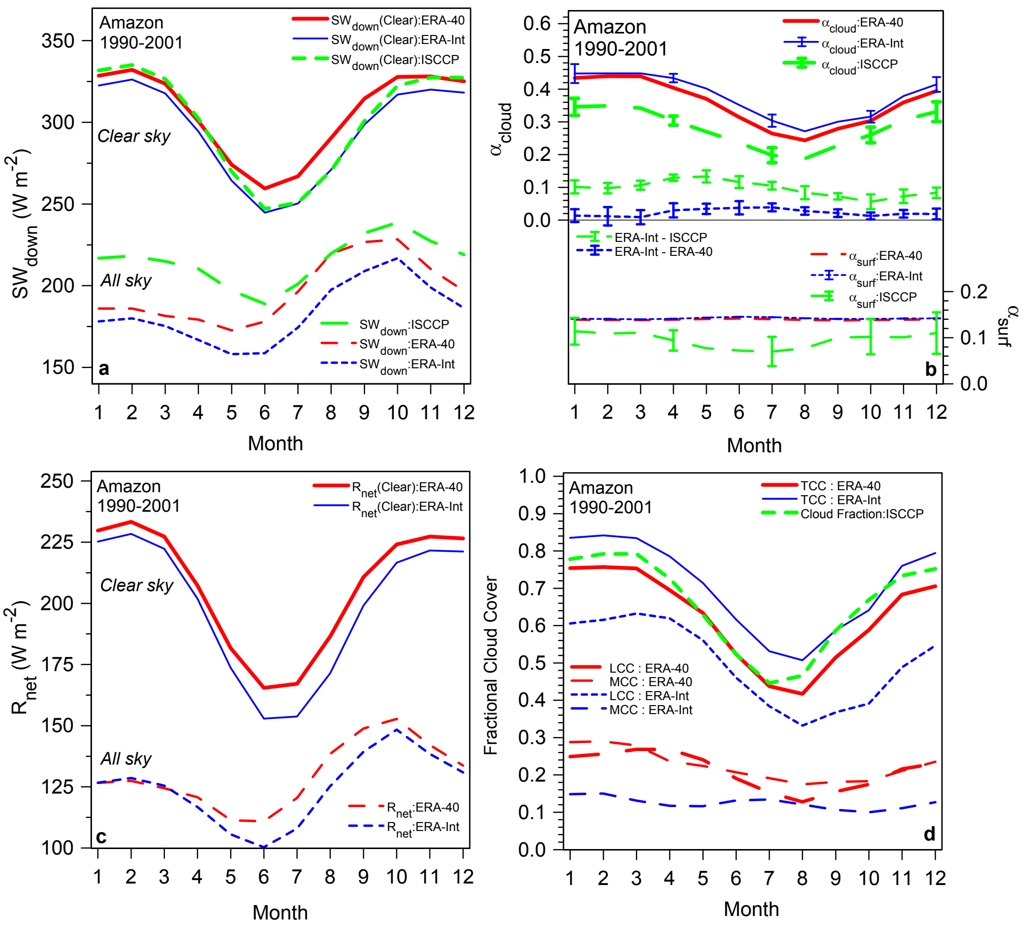

Figure 5: Mean annual cycle of (a) Clear-sky and all-sky downward short-wave flux, (b) Effective cloud albedo and surface albedo, (c) Clear-sky and all-sky net radiation, (d) Fractional cloud cover.

With this definition of effective cloud albedo, the surface net shortwave can be written in terms of two albedos

$$SW_{net} = SW_{down} - SW_{up} = (1 - \alpha_{surf})(1 - \alpha_{cloud})SW_{down}(Clear) \tag{3}$$

where the surface albedo, α_{surf}, is computed as the ratio SW_{up}/SW_{down}.

Figure 5(b) shows both these albedos for the ISCCP data and the reanalyses. Effective cloud albedo peaks in February in the rainy season and has a minimum in August in the dry season (upper curves). For the mean annual cycle, the bars show the interannual variability for the ISCCP and ERA-Interim data. The middle curves are the mean differences, ERA-Interim - ISCCP Data and ERA-Interim - ERA-40, with their standard deviations, which are small. ERA-Interim has about 1-3% greater cloud albedo than ERA-40, and 6-13% greater cloud albedo than the ISCCP data. The difference between these two curves is the difference of ERA-40 from the ISCCP data. Since the ISCCP surface shortwave cloud forcing is quite tightly constrained by the observed top-of-the-atmosphere reflected shortwave flux, it is clear that both reanalyses have too much reflective cloud, and the cloud increase from ERA-40 to ERA-Interim has increased the high bias.

The lower dashed curves show surface albedo, α_{surf}. These are similar in the reanalyses with little seasonal change and almost no interannual variability (<0.1%). In contrast, the mean ISCCP surface albedo estimate (recomputed from the monthly mean shortwave fluxes) falls from 11% in the rainy season to 7% in the dry season, a value that seems unrealistically low for the Amazon. This is the 12-year mean, and although all years

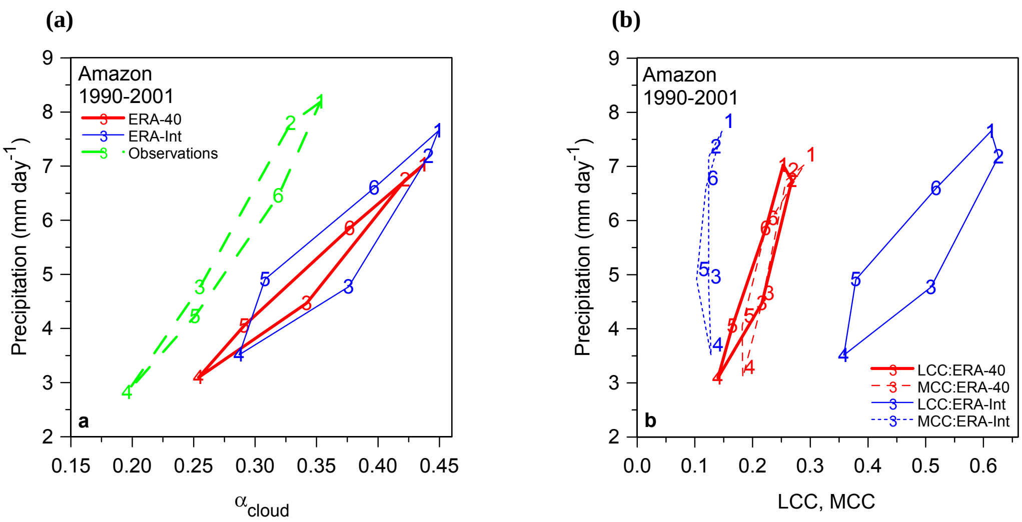

Figure 6: Mean annual cycle of relation between a) cloud albedo and precipitation; b) Low cloud and precipitation.

show a similar seasonal cycle, the standard deviation of the ISCCP interannual variability shown is large. In fact there large differences between years. For example, for the years 1992-1994, the ISCCP surface albedo falls from 15% in the rainy season to 11% in the dry season, but for the years, 1996-2000, the annual range is from 9% in the wet season to only 5% in the dry season (not shown). This reduction of 6% in the estimate of surface albedo occurs in April, 2005, when the coverage of the Amazon by the geostationary METEOSAT-3 is replaced by a GOES satellite; so the likely cause of this albedo change is the rather different spectral response of the radiometers on these two satellites (Rossow, 2008, personal communication). Zhang et al. (2007), in a detailed comparison, suggests that the uncertainty in surface broadband albedos derived from different global datasets is of order 7%. This is an area that needs more attention. For this paper, we conclude that the ISCCP data gives a more reliable observational estimate of effective cloud albedo than surface albedo.

Figure 5(c) shows the clear-sky and all-sky surface net radiation, R_{net}, for the two reanalyses. The reduction in the clear-sky net flux in ERA-Interim is dominated by the reduction in the clear-sky SW_{down} flux seen in panel (a). The all-sky net flux is substantially modified by the larger LW cloud forcing in ERA-Interim (not shown), so that the R_{net} in ERA-Interim, while lower than ERA-40 in the dry season, is barely affected in the rainy season. We do not consider the ISCCP R_{net} fluxes (not shown) to be a useful comparison, because in addition to the uncertainties in the surface albedo, the surface LWnet flux (not shown) has a significant bias. Over the Amazon the ISCCP estimate of the surface skin temperature is 5K lower than the air temperature in the rainy season, and this impacts the upward longwave flux. Probably cloud contamination is the cause of this low skin temperature bias.

Figure 5(d) compares model low cloud cover, LCC, mid-level cloud cover, MCC, and total cloud cover, TCC. ERA-Interim has about 30% more low cloud cover, LCC, than ERA-40, but less middle and high cloud (not shown), giving a smaller reduction in total cloud cover. The model changes in the boundary layer and cloud schemes in ERA-Interim have increased low cloud cover, cooled the surface and lowered cloud base substantially, with a detrimental impact on the model land-surface climate over the Amazon. The ISCCP cloud fraction estimate has a similar seasonal cycle to TCC in the reanalyses.

Comparing Figure 5(b), which is a quantitative measure of SW cloud forcing and the total fractional area of cloud in 5(d), suggests that the clouds in the reanalyses are on average optically thicker than the estimate from the ISCCP observations. An analysis for long forecasts with each intermediate model cycle shows that about two thirds of the LCC increase resulted from cycle 25R3_en, which included cloud numerics and physics and

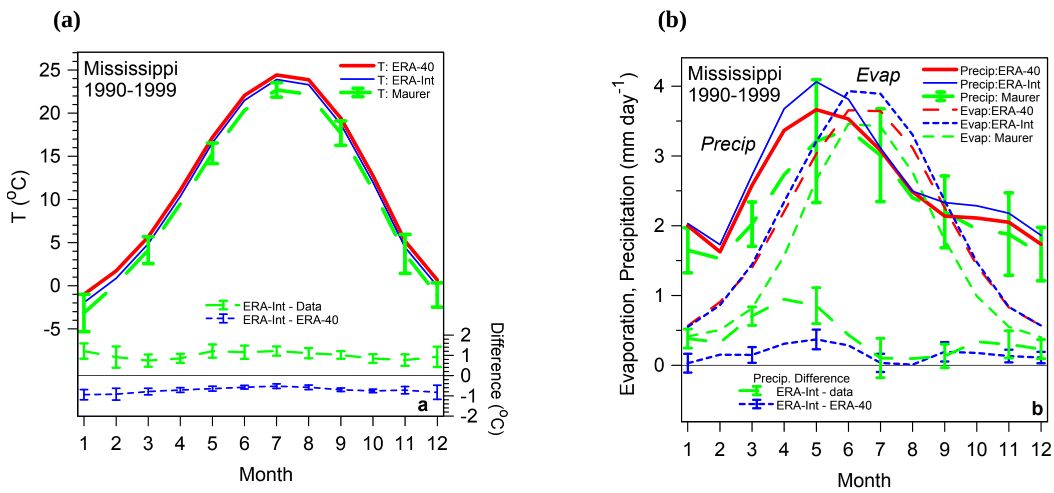

Figure 7: Mean annual cycle of (a) temperature and specific humidity (b) precipitation and evaporation for the Mississippi.

convection upgrades, and about one third from cycle 29R1, which introduced a new stratocumulus scheme (Köhler, 2005). Note that recent model cycles (later than ERA-Interim) have reduced Amazon cloud biases giving a warmer and more realistic 2-m temperature. This improvement by about 1-1.5K is mainly achieved by the cycle 32R1 radiation package McRAD involving the Monte Carlo independent column approximation (McICA) and a new solar radiation code (Morcrette et al., 2008).

Figure 6 shows that the coupling between reflective cloud and precipitation is quite different in observations and the two reanalyses. The mean annual cycle is represented by 6 points, each an average of 2 months: e.g. 1 denotes January, February, the peak of the wet season; while 4 is July, August, the peak of the dry season. Figure 6(a) shows that ISCCP α_{cloud} and observed precipitation have a tight relationship; one that is shifted to lower α_{cloud} in comparison with the reanalyses. ERA-Interim shows a broader spread of α_{cloud} over the annual cycle than ERA-40. Figure 6(b) shows that this comes from the radical change in the partition between low and mid-level cloud cover in ERA-Interim; associated with the major revisions to the cloud, convection and boundary layer schemes (discussed above and in section 1.1). There is a decrease in MCC, and a large increase in LCC (seen in Figure 5(d)), which is greater during and after the rainy season (January to June) than in the dry season (July to October).

Because α_{cloud} is directly related to SWCF through (1), Figure 6(a) shows that, over the Amazon, the ratio of the SWCF to the precipitation diabatic forcing is much smaller in the observations that the reanalyses. Section 4, later, will show that the reverse is true over the Mississippi.

2.2 Mississippi basin

For the Mississippi basin, our comparison monthly datasets are the Maurer et al. (2002) analysis for T, precipitation and evaporation from 1990-1999; and the ISCCP data for 1990-2001 for the surface shortwave fluxes and effective cloud albedo. Figure 7a (upper curves) shows the mean annual cycle, with the interannual variability shown for the Maurer data. The lower curves (right-hand-scale) show the difference of ERA-Interim from the observations and from ERA-40, and the interannual variability of these differences. ERA-Interim is a little cooler than ERA-40, an improvement, but still warmer than the temperature data from the Maurer et al. (2002) analysis. Note that the interannual variability of these differences for this mid-latitude basin are much smaller than the mean differences and smaller than the interannual variability of temperature. Specific humidity is barely changed in ERA-Interim from ERA-40 (not shown).

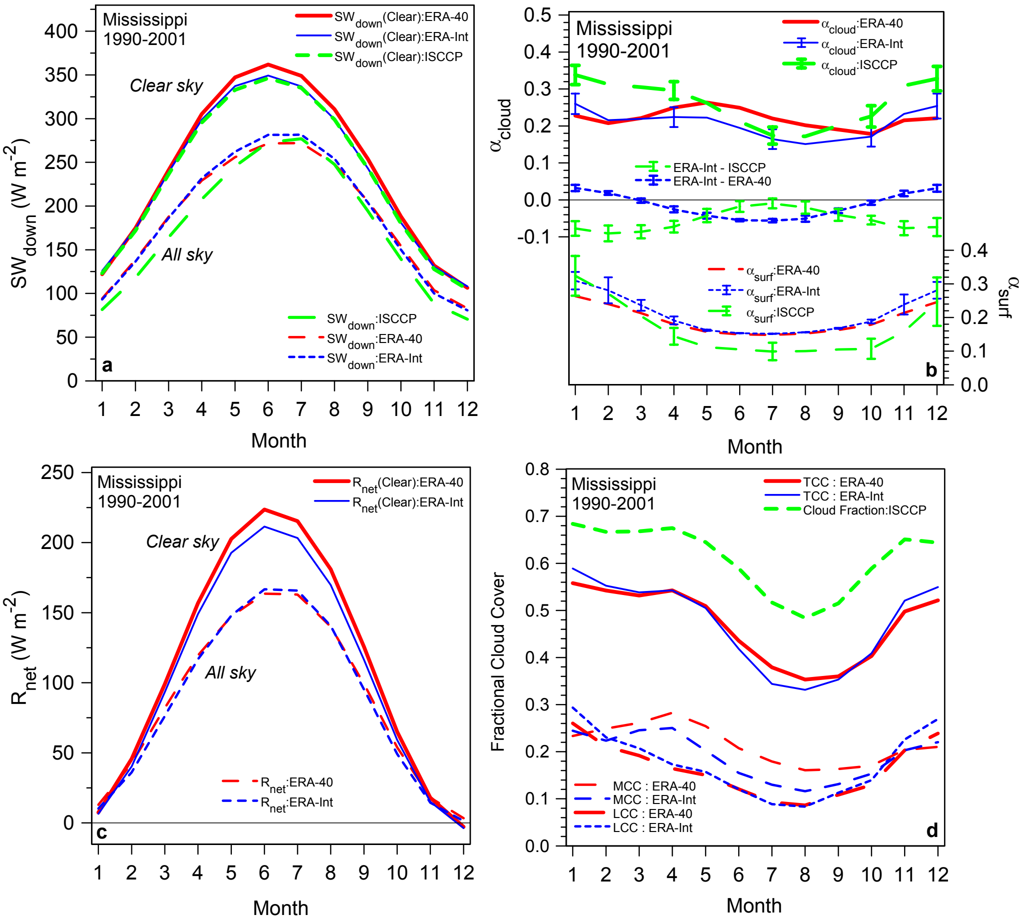

Figure 8: As Figure 5 for the Mississippi.

Figure 7b shows that ERA-Interim has more precipitation and evaporation than ERA-40, which was already greater than the Maurer data (Betts et al., 2003). The ERA-Interim precipitation differences (lower curves) are largest in April and May and very small in July and August, so that the seasonal maximum of precipitation in the reanalyses is in May, rather than as observed in June. Both reanalyses have no seasonal cycle in leaf area index, and this is one source of error in the seasonal cycle of evaporation and precipitation (Van den Hurk et al., 2003). For this mid-latitude basin (unlike for the Amazon, Figure 3), the interannual variability of the differences are much smaller than the interannual variability of precipitation, shown for the Maurer data..

Figure 8(a) and (c) show that the clear-sky SW_{down} and R_{net} fluxes are reduced in ERA-Interim, although not as much as over the Amazon, seen in the corresponding panels of Figure 5. In summer the ERA-Interim clear sky fluxes are very close to the ISCCP clear-sky flux. The surface all-sky SW_{down} estimate from the ISCCP dataset is less than the reanalyses for most of the year (Figure 8(a)).

Figure 8(b) shows the three derived effective cloud albedos. The upper curves again show the means and the interannual variability for the ISCCP and ERA-Interim data. The middle curves show the ERA-Interim differences and their interannual variability. The reduction of reflective cloud cover in ERA-Interim in summer has reduced the bias from the ISCCP data to zero in July; while the small increase in winter in ERA-Interim has also slightly reduced the bias from the data. Note that for this mid-latitude basin, the variability of the difference between ERA-Interim and ERA-40 is very small (smaller than in Figure 5(b) for the Amazon), only half the variability of the ERA-Interim - ISCCP bias. However the reflective cloud decrease in summer in

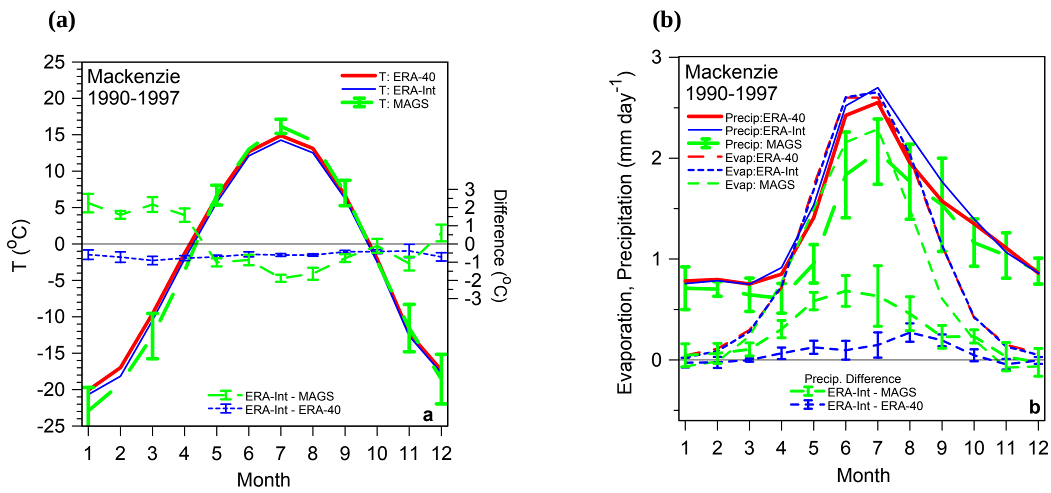

Figure 9: As Figure 7 for the Mackenzie.

ERA-Interim is associated with an increase in precipitation (Figure 7(b)). This makes the ratio of SWCF to diabatic precipitation forcing, which was low in ERA-40 (Betts, 2007), even lower in ERA-Interim (see section 4 later).

The ISCCP estimate of mean surface albedo (Figure 8(b), lower curves) is about 10% in summer, considerably less than the value used in the reanalyses (about 15%). However, again there is signifi cant interannual variability (shown by the bars). As discussed in the previous section for the Amazon, the ISCCP estimate of surface albedo is 5-6% higher for the years 1990-1992 than for 1996-2000 (not shown). The bars on surface albedo for ERA-Interim show interannual variability which is negligible in summer, but about $\pm$3% in winter because of variable snow cover.

Figure 8(c) shows that all-sky R_{net} is unchanged between the reanalyses, as the reduction in cloud in ERA-Interim cancels the reduction in the clear-sky flux. The warm season reduction in cloud cover in ERA-Interim is primarily in middle level cloud cover (MCC), not in the low cloud cover (Figure 8(d)). These changes in cloud cover between the two reanalyses over the Mississippi are quite different from the Amazon, where ERA-Interim has a large increase in low cloud cover in all months. Again the comparison of the panels (b) and (d) suggests that the clouds in the reanalyses are optically thicker than those observed by ISCCP.

2.3 Mackenzie basin

For the Mackenzie basin, our comparison datasets were prepared as a monthly climatology for the MAGS experiment: for temperature and precipitation for the period 1950-1997, and for evaporation for the period 1953-1996 (see Betts et al., 2003a). The MAGS evaporation estimates (Louie et al., 2002) are based on the method of Morton (1983). We will show averages for 1990-1997. The MAGS evaporation estimate is missing for 1997, but the impact is negligible as the interannual variability of monthly evaporation in very small in both the reanalysis and the MAGS data, of order 0.1 mm mo^{-1} in summer. Figure 9a (upper curves) shows the mean annual cycle, with the interannual variability shown for the MAGS data. The middle curves (right-hand-scale) show the difference of ERA-Interim from the observations and from ERA-40, and the interannual variability of these differences, which are much smaller than the mean biases and the interannual variability of temperature. Compared to the MAGS data, both reanalyses are warm in winter and cool in summer. ERA-Interim is slightly cooler than ERA-40 in all seasons, which is an improvement in winter, but not in summer. Specifi c humidity is barely changed in ERA-Interim from ERA-40 (not shown).

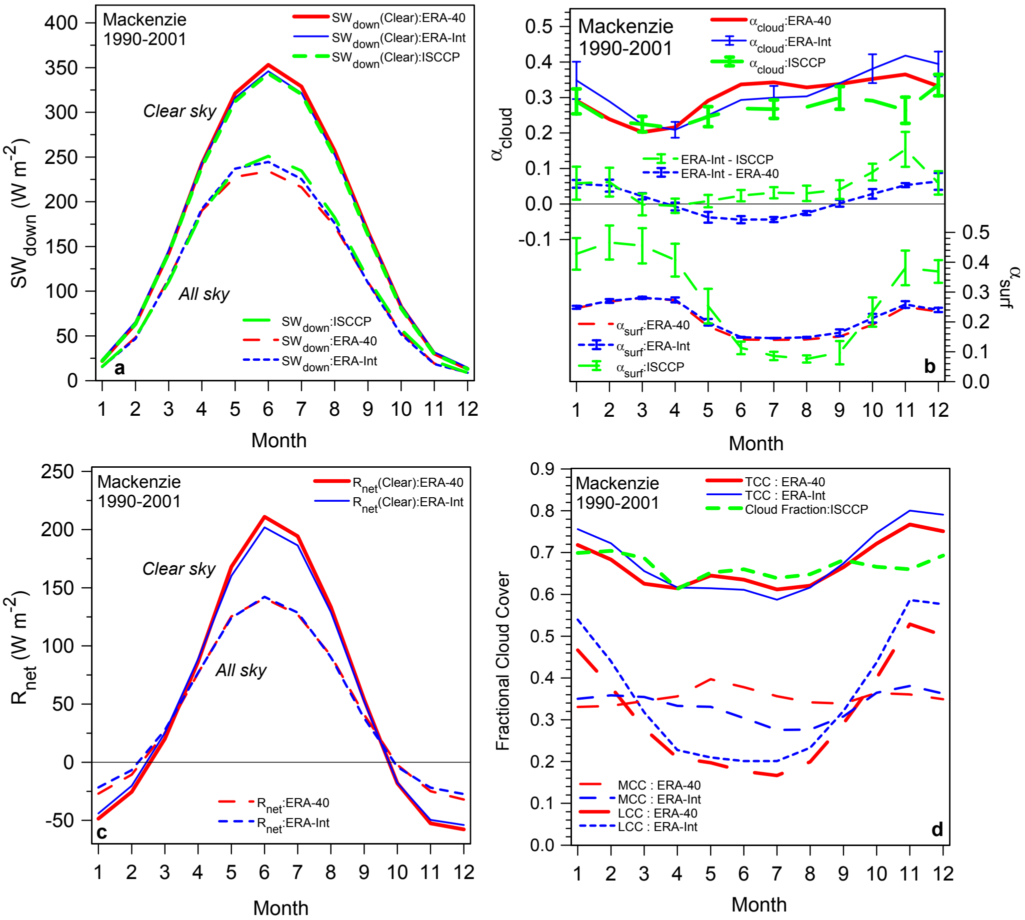

Figure 10: As Figure 8 for the Mackenzie.

Figure 9(b) shows that precipitation is slightly higher in ERA-Interim than in ERA-40, but evaporation is unchanged. Both reanalyses have more precipitation and evaporation than the MAGS data, with the largest bias in summer (lower curves). Note that in the reanalyses, summer evaporation and precipitation almost exactly balance. These changes between the two reanalyses in temperature and precipitation for the Mackenzie are qualitatively similar to those for the Mississippi.

For the surface shortwave fluxes and effective cloud albedo, we again compare with the ISCCP data for the period 1990-2001. Figures 10(a) and (c) show that ERA-Interim has reduced clear-sky SW_{down} and R_{net} in the warm season, although for this northern basin the reductions are smaller than we have seen for both the Amazon and Mississippi. However the surface all-sky SW_{down} in ERA-Interim is greater than in ERA-40 in summer. For both clear and all-sky SW_{down}, ERA-Interim is closer to the ISCCP observations in summer (Figure 10(a)).

As with the Mississippi, ERA-Interim has less reflective cloud in summer and more in winter than ERA-40 (Figure 10(b)). This results in a rather small bias in effective cloud albedo in ERA-Interim, except in winter, when the impact on shortwave cloud forcing is however small. The ISCCP surface albedo has a much wider range, 8% in summer to 48% in winter, than the reanalyses, whose summer to winter range is only 14-28%. The differences in all-sky R_{net} are tiny (Figure 10(c)) except in mid-winter, when the longwave contributions dominate, giving a smaller surface cooling in ERA-Interim. As over the Mississippi, the fall in cloud cover in summer is primarily due to a reduction in mid-level cloud (Figure 10(d)).

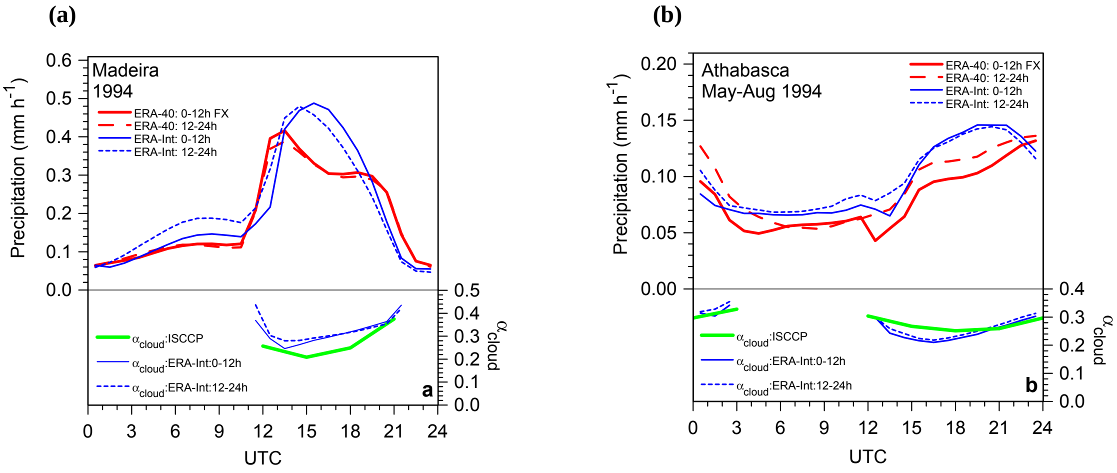

Figure 11: Diurnal cycle of precipitation for the 0-12h and 12-24h FX for ERA-40 and ERA-Interim for (a) Madeira and (b) Athabasca. Lower curves are diurnal cycle of daytime cloud albedo for the 0-12h and 12-24h FX for ERA-Interim and ISCCP observations.

3 Diurnal Cycle

Figure 11 shows the differences in the mean diurnal cycle of precipitation between ERA-40 and ERA-Interim for the Madeira River (south-western sub-basin, 42, of the Amazon in Figure 1); and for the Athabasca River (south-eastern basin, 33, of the Mackenzie River in Figure 1). The lower curves compare the daytime cloud albedo for the ISCCP observations and ERA-Interim (the hourly clear-sky shortwave fluxes needed to calculate effective cloud albedo were not included in the river-basin archive for ERA-40). Over the Amazon, ERA-40 had a spurious sharp precipitation peak soon after sunrise (Betts and Jakob, 2002). The convective parameterization scheme, which tested lifted surface parcels for instability, activated as soon as the night-time stable boundary layer was eroded. In ERA-Interim, the scheme was changed to lift thicker layers (Bechtold et al., 2004) and this delays the onset of convective precipitation by about two hours. However this precipitation peak, just before local noon (1400 UTC) in the 0-12h forecast (FX), and an hour earlier in the 12-24h FX, is still too early in the diurnal cycle. For ERA-Interim, we see a spinup of precipitation at night and a spin-down in the daytime in Figure 11(a). Over the Amazon as a whole (not shown), ERA-40 has a very small spin-down of daily precipitation (less than 2% between the 0-12h and 12-24h FX), and in ERA-Interim this spin-down is even smaller (less than 1%). The lower curves show that ERA-Interim has systematically a greater cloud albedo than ISCCP during daylight, consistent with the monthly data for the whole Amazon basin shown in Figure 5(b).

Figure 11(b) for the Athabasca shows the differences in the diurnal cycle of precipitation between the reanalyses in the warm season (May to August) at high latitudes. ERA-40 has an evening precipitation peak, while ERA-Interim has a precipitation peak which is near local noon (1800 UTC). ERA-40 has a significant spinup of precipitation, about 15% between the 0-12h FX and 12-24h FX (see also Betts et al., 2003a). The corresponding spinup of precipitation in ERA-Interim is much less, of order 5%, for both the Mackenzie (and the Mississippi, not shown). The improved humidity analysis and the 4-D variational assimilation system in ERA-Interim are responsible for this improvement. For this sub-basin of the Mackenzie, the lower curves in Figure 11(b) show that the bias in cloud cover between ERA-Interim and the ISCCP data is small.

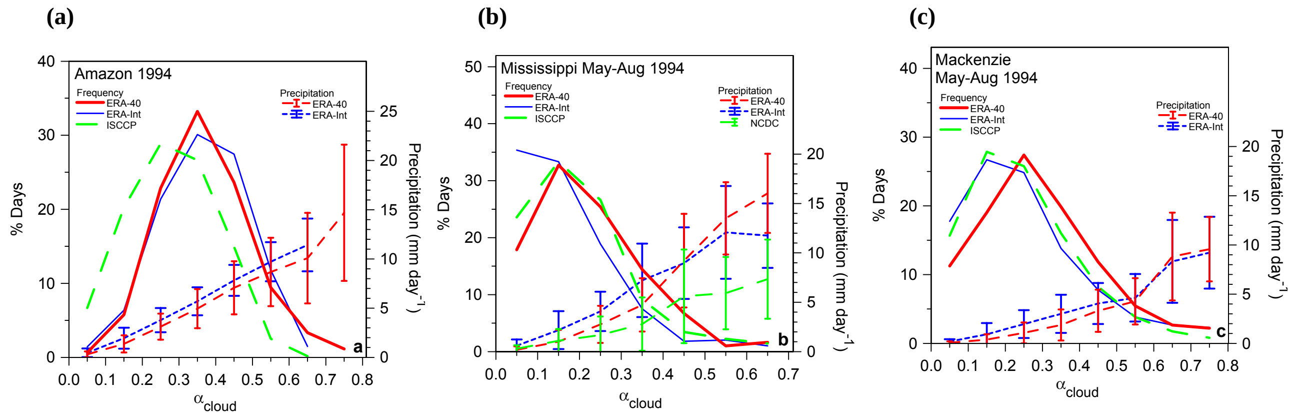

Figure 12: Percent of days and precipitation as a function of cloud albedo for (a) Amazon (b) Mississippi and (c) Mackenzie.

4 Daily Cloud statistics and coupling of precipitation to cloud albedo

In Figure 12(a) the daily mean data for all 5 Amazon sub-basins has been binned by effective cloud albedo. The frequency distribution of days in ERA-40, ERA-Interim and the ISCCP data with a given cloud albedo are compared (left-hand-scale). The differences shown in Figure 5 on the monthly timescale are reflected here. In comparison with ERA-40, the ISCCP data distribution is shifted substantially to lower cloud albedo values, while the distribution for ERA-Interim is shifted slightly to the right. Model precipitation, binned by model cloud albedo (right-hand-scale), increases quasi-linearly with cloud albedo (and the SW cloud forcing), but the two reanalyses differ. The standard deviations in ERA-Interim are smaller, meaning that the coupling between precipitation and cloud albedo is tighter in ERA-Interim. The upward shift of the ERA-Interim precipitation curve (although within the standard deviations) means that the ratio of the surface SWCF (see equation (1)) to the precipitation heating of the atmosphere is slightly smaller in ERA-Interim than ERA-40. We do not have daily precipitation data averaged over the Amazon for comparison, but it was clear from the monthly data in Figure 6(a), that this important climate ratio is far smaller in the observations than both reanalyses.

Four basins of the Mississippi (Red-Arkansas, Missouri, Upper Mississippi and Ohio-Tennessee, which are basins 29-32 in Figure 1) are combined for the warm season months, May - August, in Figure 12(b). The shift towards lower cloud cover in ERA-Interim, seen in summer in Figure 8(b), appears as a distribution shift with many more nearly cloud-free days in ERA-Interim, more than are seen in the ISCCP data. For the precipitation comparison on the right-hand-scale, we have added daily precipitation, derived by Betts (2007) from the Higgins et al. (1996, 2000) datasets. Although the standard deviations are large, it is clear that the two reanalyses and the observations have quite different relationships. For a given precipitation, reflective cloud cover in the reanalyses is too low compared to observations. As noted in Betts (2007), this means that the ratio of the surface SWCF to the diabatic precipitation forcing is too low in ERA-40; and for α_{cloud}¡0.45, it is still lower in ERA-Interim.

Figure 12(c) is the corresponding distribution of cloud cover and precipitation for the 7 sub-basins of the Mackenzie. The shift in the distributions from ERA-40 to ERA-Interim is similar to that seen for the Mississippi. However, the reduction in cloud cover in the warm season in ERA-Interim now gives a distribution that is close to the ISCCP distribution. We do not have daily precipitation for the Mackenzie for comparison.

5 Summary and Conclusions

There have been significant improvements in the global hydrological cycle in terms of water vapor, clouds and precipitation in ERA-Interim versus ERA-40, especially over the oceans (Uppala et al., 2008). This paper has looked in more detail at some of the differences between observations, ERA-40 and ERA-Interim over three large river basins, the Amazon, Mississippi and Mackenzie. For the Amazon, precipitation has increased in ERA-Interim, although the amplitude of the seasonal cycle of precipitation remains too low. The diurnal cycle of precipitation has improved in that the spurious peak after sunrise has gone in ERA-Interim, but the precipitation maximum a little before local noon is still too early in the diurnal cycle. The new humidity analysis appears to have removed the interannual drift in precipitation seen in ERA-40 over the Amazon. However changes to the boundary layer and cloud schemes have increased low cloud cover by about 30%; and the small cold bias in ERA-40 of -0.3 K over the Amazon has increased substantially in ERA-Interim to -1.7 K. Low cloud cover over land is difficult to simulate because of the following positive feedback: more LCC cools the surface, which lowers the lifting condensation level, which generally gives more cloud.

The atmospheric shortwave reflection is also greater in ERA-Interim, and in the dry season (June to August) the downwelling shortwave clear-sky flux has decreased by 16 Wm $^{-2}$, closer to the ISCCP observations than ERA-40. The effective cloud albedo is 1-3% higher in ERA-Interim than ERA-40, and 6-13% higher than values derived from the ISCCP downwelling shortwave observations during the annual cycle. As a result the ratio of the surface short wave cloud forcing to the precipitation heating of the atmosphere is much lower in the observations than both reanalyses.

For the Mississippi basin, both precipitation and evaporation exceeded the Maurer et al. (2002) estimates in ERA-40, and both have increased further in ERA-Interim. The basin mean temperature is slightly lower in ERA-Interim, and a little closer to observations. Except in summer, ERA-40 has less reflective cloud than the ISCCP observations. In ERA-Interim, cloud cover has decreased in the warm season, so this reanalysis has less cloud than the observations in all months except July; and substantially more days with nearly clear skies from May to August. The ratio of the surface shortwave cloud forcing to the precipitation heating of the atmosphere is lower in ERA-40 than the observations in the warm season (Betts, 2007) and it is generally still lower in ERA-Interim.

For the Mackenzie basin, the differences between the reanalyses are for the most part similar to those for the Mississippi basin. For temperature, ERA-Interim is a little cooler, which, compared with observations, gives a smaller warm bias in winter, but a slightly larger cool bias in summer. The differences in the clear-sky shortwave fluxes decrease systematically towards higher latitudes, and they are much smaller over the Mackenzie than in the tropics. For the Mackenzie, a reduction in summer cloud cover from ERA-40 gives a better fit to the ISCCP data.

One systematic improvement in ERA-Interim in mid-latitudes is that the spinup of precipitation in the first 24h of forecasts, which was 15% or more in ERA-40, has been reduced to about 5%. The improved humidity analysis and the 4-D variational assimilation system in ERA-Interim are responsible for this improvement.

We have compared the performance of two reanalyses over three large river basins in the Americas, evaluating primarily temperature, precipitation and shortwave radiation against observations. The changes between the reanalyses are quite different in tropics and mid-latitudes. In some aspects, such as reduced spinup of the precipitation in mid-latitudes, reduced drift of precipitation in the tropics and some improvement in the diurnal cycle in the tropics, ERA-Interim is clearly superior. However; the increase of cloud cover and reduction of the surface shortwave flux over the Amazon is unrealistic and gives a substantial cold 2-m temperature bias.

ERA-Interim is expected to reach real time at the end of 2008 and will then continue as a climate data assimilation system. The ERA-Interim data is available at a resolution of 1.5deg on the ECMWF data services web page. The model development cycles of course continue. Recent model cycles (later than cycle 31R2 used in ERA-Interim) have reduced Amazon cloud biases, giving a warmer and more realistic 2-m temperature, and the low cloud bias over North America has been halved in the currently operational cycle 33R1.

Acknowledgements

Alan Betts acknowledges support from NSF under grant ATM0529797, and from NASA under NEWS grant NNG05GQ88A. We are grateful for the help of Dick Dee and Sakari Uppala at ECMWF. Especial thanks to Aguio Dai for the processed Amazon datasets, to Bill Rossow for the ISCCP data, to Ed Maurer and to Mike Bosilovich for the processed Mississippi datasets, and to Robert Crawford, the MAGS data manager.

References

Andersson, E., P. Bauer, A. Beljaars, F. Chevallier, E. Hólm, M. Janisková, P. Kållberg, G. Kelly, P. Lopez, A. Mcnally, E. Moreau, A. J. Simmons, J-N. Thépaut and A. M. Tompkins (2005). Assimilation and Modeling of the Atmospheric Hydrological Cycle in the ECMWF Forecasting System, *Bull. Amer. Meteorol.* Soc., **86**, 387-402.

Bechtold, P., J.-P. Chaboureau, A. Beljaars, A. K. Betts , M. Miller, M. Köhler, M. Miller and J.-L. Redelsperger (2004). The simulation of the diurnal cycle of convective precipitation over land in a global model. *Q. J. R. Meteorol. Soc.*, **130**, 3119-3137.

Beljaars, A., A. Brown and N. Wood (2003). A new parametrization of turbulent orographic form drag. *ECMWF Tech. Memo*, **427**, available at http://www.ecmwf.int/publications.

Betts, A. K. (2007). Coupling of water vapor convergence, clouds, precipitation, and land-surface processes, *J. Geophys. Res.*, **112**, D10108, doi:10.1029/2006JD008191.

Betts, A. K and P. Viterbo (2005). Land-surface, boundary layer and cloud-field coupling over the south-western Amazon in ERA-40. *J. Geophys. Res.*, **110**, D14108, doi:10.1029/2004JD005702.

Betts, A. K., J. H. Ball and P. Viterbo (2003a). Evaluation of the ERA-40 surface water budget and surface temperature for the Mackenzie River basin. *J. Hydrometeorology*, **4**, 1194-1211.

Betts, A. K., J. H. Ball, M, Bosilovich, P. Viterbo, Y.-C. Zhang, and W. B. Rossow (2003b). Intercomparison of Water and Energy Budgets for five Mississippi Sub-basins between ECMWF Reanalysis (ERA-40) and NASA-DAO fvGCM for 1990-1999. *J. Geophys. Res.*, **108** (D16), 8618, doi:10.1029/2002JD003127.

Betts, A. K, J.H., Ball, P. Viterbo, A. Dai and J. A. Marengo (2005). Hydrometeorology of the Amazon in ERA-40. *J. Hydrometeorology*. **6**, 764-774.

Betts, A.K., C. Jakob (2002). Evaluation of the diurnal cycle of precipitation, surface thermodynamics, and surface fluxes in the ECMWF model using LBA data. *J. Geophys. Res.*, **107**, (D20). 8045, doi:10.1029/2001JD000427.

Dai, A., K. E. Trenberth, and T. Qian (2004). A global dataset of Palmer severity index for 1870-2002: Relationship with soil moisture and effects of surface warming. *J. Hydrometeor.*, **5**, 1117-1130.

Dai, A. (2006). Recent climatology, variability and trends in global surface humidity. *J. Climate*, **19**, 3589-3606.

Hagemann, S., K. Arpe amd L. Bengtsson (2005). Validation of the hydrological cycle of ERA-40. *ERA-40 Project Report Series* No. **24**, ECMWF, available at http://www.ecmwf.int/publications.

Higgins, R.W., J.E. Janowiak and Y.-P. Yao (1996). A gridded hourly precipitation database for the United States (1963-1993).*NCEP/Climate Prediction Center Atlas*, **1**, Natl. Weather Serv., NOAA, U.S. Dep. of Commer., Washington, D.C.

Higgins, R.W., W. Shi, E. Yarosh and R. Joyce (2000). Improved United States precipitation quality control system and analysis, *NCEP/Climate Prediction Center Atlas*, **7**, Natl. Weather Serv., NOAA, U.S. Dep. of Commer., Washington, D.C.

Jones, P. D., and A. Moberg (2003). Hemispheric and large-scale surface air temperature variations: An extensive revision and an update to 2001. *J. Climate*, **16**, 206-223.

Kållberg, P., A. Simmons, S. Uppala and M. Fuentes (2004). The ERA-40 archive. *ERA-40 Project Report Series* No. **17** (Revised October 2007), available at http://www.ecmwf.int/publications.

Köhler, M. (2005). Improved prediction of boundary layer clouds. *ECMWF Newsletter*, **104**, 18-22, available at http://www.ecmwf.int/publications/newsletters.

Louie, P. Y. T., W. D. Hogg, M. D. MacKay, X. Zhang, and R. Hopkinson (2002). The water balance climatology of the Mackenzie basin with reference to the 1994/95 water year. *Atmos.-Ocean*, **40**, 159-180.

Maurer, E.P., A.W. Wood, J.C. Adam, D.P. Lettenmaier, and B. Nijssen (2002). A Long-Term Hydrologically-Based Data Set of Land Surface Fluxes and States for the Conterminous United States, *J. Climate*, **15**, 3237-3251.

Morcrette, J.-J, P. Bechtold, A. Beljaars, A. Benedetti, A. Bonet, F. Doblas-Reyes, J. Hague, M. Hamrud, J. Haseler, J.W. Kaiser, M. Leutbecher, G. Mozdzynski, M. Razinger, D. Salmond, S. Serrar, M. Suttie, A. Tompkins, A. Untch and A. Weisheimer (2007). Recent advances in radiation transfer parametrizations. *ECMWF Tech. Memo*, **539**, available at http://www.ecmwf.int/publications.

Morcrette, J.-J, H. Barker, J. Cole, M. Iacono and R. Pincus (2008). Impact of a new radiation package, McRAD, in the ECMWF Integrated Forecasting System. *Mon. Wea. Rev.* (in press).

Morton, F. I. (1983). Operational estimates of areal evapotranspiration and their significance to the science and practice of hydrology. *J. Hydrol.*, **66**, 1-76.

Rossow, W. B., and Y.-C. Zhang (1995). Calculation of surface and top-of-atmosphere radiative fluxes from physical quantities based on ISCCP: 2. Validation and first results, *J. Geophys. Res.*, **100**, 1167-1197.

Simmons, A. J., P. D. Jones, V. da Costa Bechtold, A. C. M. Beljaars, P. W. Kållberg, S. Saarinen, S. M. Uppala, P. Viterbo, and N. Wedi (2004). Comparison of trends and low-frequency variability in CRU, ERA-40, and NCEP/NCAR analyses of surface air temperature, *J. Geophys. Res.*, **109**, D24115, doi:10.1029/2004JD005306.

Simmons, A., S. Uppala, D. Dee and S. Kobayashi (2006). ERA-Interim: New ECMWF reanalysis products from 1989 onwards, *ECMWF Newsletter*, **110**, 25-35, available at http://www.ecmwf.int/publications.

Tompkins, A. M., P. Bechtold, A. C. M. Beljaars, A. Benedetti, S. Cheinet, M. Janisková, M. Köhler, P. Lopez, and J.-J. Morcrette (2004). Moist physical processes in the IFS: Progress and Plans. *ECMWF Tech. Memo*, **452**, 93 pp., available at http://www.ecmwf.int/publications.

Uppala, S.M., Kållberg, P.W., Simmons, A.J., Andrae, U., da Costa Bechtold, V., Fiorino, M., Gibson, J.K., Haseler, J., Hernandez, A., Kelly, G.A., Li, X., Onogi, K., Saarinen, S., Sokka, N., Allan, R.P., Andersson, E., Arpe, K., Balmaseda, M.A., Beljaars, A.C.M., van de Berg, L., Bidlot, J., Bormann, N., Caires, S., Chevallier, F., Dethof, A., Dragosavac, M., Fisher, M., Fuentes, M., Hagemann, S., Hólm, E., Hoskins, B.J., Isaksen, L., Janssen, P.A.E.M., Jenne, R., McNally, A.P., Mahfouf, J.-F., Morcrette, J.-J., Rayner, N.A., Saunders, R.W., Simon, P., Sterl, A., Trenberth, K.E., Untch, A., Vasiljevic, D., Viterbo, P., and J. Woollen (2005). The ERA-40 re-analysis. *Quart. J. R. Meteorol. Soc.*, **131**, 2961-3012.doi:10.1256/qj.04.176.

Uppala, S., D. Dee, S. Kobayashi, P. Berrisford and A. Simmons (2008). Towards a climate data assimilation system: status update of ERA-Interim, *ECMWF Newsletter*, **115**, 12-18, available at `http://www.ecmwf.int/publications`.

Van den Hurk, B.J.J.M., P. Viterbo, A.C.M. Beljaars and A. K. Betts (2000). Offline validation of the ERA40 surface scheme. *ECMWF Tech. Memo*, **295**, 43 pp., available at `http://www.ecmwf.int/publications`.

Van den Hurk, B.J.J.M., P. Viterbo and S.O. Los (2003). Impact of leaf area index seasonality on the annual land surface evaporation in a global circulation model. *J. Geophys. Res.*, **108**, D6, 4191, doi:10.1029/2002JD002846.

Woo, M-k, W.R. Rouse, R.E. Stewart and J.M.R. Stone (2008). The Mackenzie GEWEX study: a contribution to cold region atmospheric and hydrologic sciences. Chapter 1 in *Cold Region Atmospheric and Hydrologic Studies, The Mackenzie GEWEX Experience. Vol 1: Atmospheric Dynamics*, M-k. Woo, Editor, Springer, ISBN 978-3-540-73935-7.

Zhang, Y.-C., W. B. Rossow, and A. A. Lacis (1995). Calculation of surface and top-of-atmosphere radiative fluxes from physical quantities based on ISCCP: 1. Method and sensitivity to input data uncertainties, *J. Geophys. Res.*, **100**, 1149-1165.

Zhang, Y.-C., W. B. Rossow, A. A. Lacis, V. Oinas and M. I. Mishchenko (2004). Calculation of radiative fluxes from the surface to top of atmosphere based on ISCCP and other global data sets: Refinements of the radiative transfer model and the input data. *J. Geophys. Res.*, **109**, D19105, doi:10.1029/2003JD004457.

Zhang, Y.-C., W. B. Rossow and P. W. Stackhouse, Jr., (2006). Comparison of different global information sources used in surface radiative flux calculation: Radiative properties of the near-surface Atmosphere. *J. Geophys. Res.*, **111**, D13106, doi:10.1029/2005JD006873.

Zhang, Y.-C., W. B. Rossow and P. W. Stackhouse, Jr., (2007). Comparison of different global information sources used in surface radiative flux calculation: Radiative properties of the surface. *J. Geophys. Res.*, **111**, D01102, doi:10.1029/2005JD007008.